

Two channel orbital Kondo effect in quantum dot with $SO(n)$ symmetry

T. Kuzmenko¹, K. Kikoin² and Y. Avishai^{1,3}

¹*Department of Physics, Ben Gurion University of the Negev, Beer Sheva 84105, Israel*

²*Raymond and Beverly Sackler Faculty of Exact Sciences,*

School of Physics and Astronomy, Tel Aviv University, 69978 Tel Aviv, Israel

³*Department of Physics, Hong Kong University of Science and Technology, Clear Water Bay, Kowloon, Hong Kong*

A scenario for the formation of symmetry protected non-Fermi-liquid (NFL) Kondo effect (KE) with spin variable enumerating Kondo channels is suggested and worked out. In doubly occupied symmetric triple quantum dot within parallel geometry, the NFL low-energy regime arises provided the device possesses both source-drain and left-right parity. Kondo screening follows a multistage renormalization group mechanism: reduction of the energy scale is accompanied by the change of the relevant symmetry group from $SO(8)$ to $SO(5)$. At low energy, three phases compete: 1) under-screening spin triplet (conventional) KE; 2) spin singlet potential scattering; 3) NFL phase where the roles of spin and orbital degrees of freedom are swapped.

I. MAIN RESULTS

The physics of two-channel Kondo effect (KE) that is marked by non-fermi liquid (NFL) behavior at low temperatures has been with us for more than three decades¹. Most attempts to realize it in complex quantum dots (CQD) failed because interference between two channels is virtually unavoidable, leading to channel anisotropy and to an instability of the two-channel fixed point. To remedy this instability, a suppression of interchannel co-tunneling is attempted, using special design of the CQD. Apparently, the most successful attempt is realized in double quantum dot (DQD)², where the interference is suppressed by Coulomb blockade. Another design which allows one to (at least) approach the elusive two-channel fixed point was suggested in Ref.³, based on a structure composed of triple quantum dot (TQD) in serial geometry (Fig. 1a). Here, the strong Coulomb blockade in the central dot minimizes (but does not completely eliminate) interchannel interference.

Yet another approach for achieving NFL two-channel Kondo regime is to swap the roles of charge and spin variables, i.e. to treat orbital or charge fluctuations as pseudospin variables causing Kondo screening, whereas spin projection quantum numbers serve as different channels⁴⁻⁶. The idea of accessing the NFL two-channel Kondo regime in "natural" two-level systems in heavy particles was subject to criticism⁷⁻⁹. In these systems, pseudospin-flip is a generic tunneling process with a characteristic (long) time t_{tun} , unlike real spin flip processes which are practically instantaneous. As a result the ultraviolet cutoff for Kondo effect is the energy $\sim \hbar/t_{\text{tun}}$. This energy is of the order of the distance to the next excited level in two-well potential. The latter interval is much smaller than the energy scale ε_F for "light" electrons. As a result the energy interval available for the formation of the logarithmic singularity is too narrow and the resulting Kondo temperature is very small $T_K \ll \Delta$ where Δ is the depth of the occupied level in the well relative ε_F . Thus the strong coupling regime remains in fact unattainable as far as two-level systems in heavy

particles serve as pseudospin.

Natural and artificial nano-objects provide their own mechanisms of two-channel Kondo tunneling assisted by pseudospin excitations. One such mechanism was proposed for a "quantum box" connected to a lead by a single-mode point contact^{10,11}. In this case the relevant operator which logarithmically scales the crossover from the high temperature to the low-temperature region is the capacitance $C(T) \sim \ln(T/T_K)$. In another model with $SU(3)$ dynamical symmetry the excited state with parity-degenerate rotational levels ($m = \pm 1$) may cross the $m = 0$ level due to interaction with a bath and thus become the source of orbital KE with spin playing part of tunneling channel¹².

In this work we offer a relatively simple realization of over-screened orbital Kondo effect where the two-channel regime is realized by two spin projections. The proposed device is composed of a doubly occupied TQD in contact with two terminals within parallel geometry³. It will be shown that the present model is free of the shortcomings pointed out in Refs.⁷⁻⁹ and that the role of higher excited levels is completely different. Experimentally, this configuration may be realized in triangular arrangement of vertical dots¹³ (see Fig 1b). The TQD is doubly

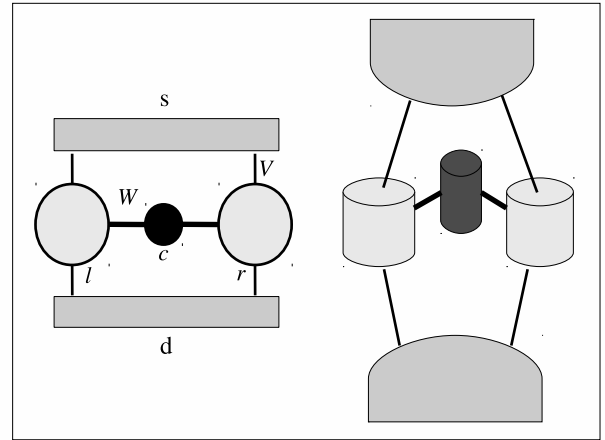


FIG. 1: Axially symmetric triple quantum dot in planar (left panel) and vertical (right panel) geometries.

occupied in the ground state, and only singly occupied states are involved in cotunneling processes. A state $|\lambda\rangle$ of the *isolated* TQD (with corresponding energy E_λ), can be either $|\sigma\rangle=|\pm\frac{1}{2}\rangle$ or $|\Lambda\rangle=|00\rangle$ (singlet), $|1\mu\rangle$ (triplet) for a TQD occupied by either $N=1$ or $N=2$ electrons respectively (see below).

The starting point is an Anderson-like tunneling Hamiltonian, $H = H_b + H_d + H_{\text{tun}}$ where

$$H_b = \sum_{i=l,r} \sum_{k\sigma} \sum_{a=e,o} \varepsilon_k c_{iak\sigma}^\dagger c_{iak\sigma}, \quad H_d = \sum_{\lambda=\sigma,\Lambda} E_\lambda |\lambda\rangle\langle\lambda|$$

$$H_{\text{tun}} = \sqrt{2} \sum_{ik\sigma\sigma'\Lambda} \sigma' \left(V_\Lambda c_{iek\sigma}^\dagger |\bar{\sigma}'\rangle\langle\Lambda| + \text{H.c.} \right) + \text{H.c.} \quad (1)$$

Here, assuming configurations having both left-right (l - r) and source-drain (s - d) symmetry, the operators $c_{iak\sigma}^\dagger = (c_{isk\sigma}^\dagger \pm c_{idk\sigma}^\dagger)/\sqrt{2}$ are even and odd combinations of source and drain electron operators. The tunneling amplitudes $V_\Lambda = \langle\Lambda|V|\bar{\sigma}',iek\sigma\rangle$ between the dot and the leads depend on the two-electron state Λ of the TQD¹⁶.

The low-energy spectrum E_Λ of the isolated doubly occupied TQD consists of two spin doublets E_{S_i} and two spin triplet E_{T_i} ($i = g, u$ for even and odd combinations of l and r states). (see Appendix for detailed descrip-

tion renormalization¹⁴⁻¹⁷ implies that all the levels flow downwards with scaling invariants,

$$E_\Lambda^* = E_\Lambda(D) - \pi^{-1} \Gamma_\Lambda \ln(D/\Gamma_\Lambda). \quad (2)$$

Here $\Gamma_\Lambda = \pi\rho_0|V_\Lambda|^2$ is the tunneling rate for the state $|\Lambda\rangle$, $\ln(D/D_0) \equiv \eta$ is the scaling variable and D_0 is the conduction bandwidth $-D_0/2 \leq \varepsilon_k \leq D_0/2$. The renormalization rates Γ_Λ/π depend crucially on Λ , and the scaling trajectories $E_\Lambda(D)$ intersect as in Fig. 2 due to the inequality $\Gamma_{T_g} > \Gamma_{S_u} > \Gamma_{T_u} > \Gamma_{S_g}$ (see Appendix for details). Various scenarios of multistage Kondo effect are possible, including that illustrated by the flow diagram of Fig. 2, where the level E_{S_u} crosses level E_{T_u} before the level E_{T_g} "overtakes" both of them. There is a window of input parameters, where the orbital KE emerges due to nearly degenerate orbital doublet/spin singlet forming as a result of Haldane flow at $D \approx \bar{D}$, where charge fluctuations are frozen. At this stage, an application of the Schrieffer-Wolff (SW) transformation generates the effective spin Hamiltonian for $N = 2$ channels, and further RG transformation follows Anderson's poor-man scaling procedure for renormalization of the exchange constants¹⁸.

The full $SO(8)$ spin Hamiltonian H_{SW} is written in¹⁶. From Fig. 2 we conclude that the poor-man scaling procedure should take into account the evolution of dynamical symmetry along the chain $SO(8) \rightarrow SO(5) \rightarrow$ orbital $SU(2)$. To illustrate the key points of transformation from spin KE to orbital KE, we consider the simplified picture, where only one of the two triplets is taken into account, i.e. write down the spin Hamiltonian pertaining to the part relevant to the KE for $SO(5)$ multiplet composed of one triplet T_u and two singlets S_u and S_g .

$$H_{\text{SW}} = \sum_{\mu} \bar{E}_{T_u} X^{T_u\mu, T_u\mu} + \sum_{\eta=u,g} \bar{E}_{S_\eta} X^{S_\eta S_\eta} + \quad (3)$$

$$J_1 \mathbf{S}_u \cdot \mathbf{s}_{uu} + J_2 \mathbf{R}_u \cdot \mathbf{s}_{uu} + J_3 (\mathbf{R}_{ug}^{(1)} \cdot \mathbf{s}_{gu} + \mathbf{R}_{gu}^{(2)} \cdot \mathbf{s}_{ug}).$$

Here $\mu = 1, 0, \bar{1}$ are projections of spin $S = 1$, the levels \bar{E}_Λ are renormalized in accordance with (2). The group generators forming the o_5 algebra are three vectors $\mathbf{S}_u, \mathbf{R}_u, \tilde{\mathbf{R}} = \mathbf{R}_{ug}^{(1)} + \mathbf{R}_{gu}^{(2)}$ and the scalar A :

$$S_u^+ = \sqrt{2}(X^{1_u 0_u} + X^{0_u \bar{1}_u}), \quad S_u^z = X^{1_u 1_u} - X^{\bar{1}_u \bar{1}_u},$$

$$R_u^+ = \sqrt{2}(X^{1_u S_u} - X^{S_u \bar{1}_u}), \quad R_u^z = -(X^{0_u S_u} + X^{S_u 0_u}),$$

$$\tilde{R}^+ = \sqrt{2}(X^{1_u S_g} - X^{S_g \bar{1}_u}), \quad \tilde{R}^z = -(X^{0_u S_g} + X^{S_g 0_u}),$$

$$A = i(X^{S_u S_g} - X^{S_g S_u}). \quad (4)$$

\mathbf{s}_{ij} are the components of local spin operators for even and odd partial waves of the band electrons, $\mathbf{s}_{ij} = \frac{1}{2} \sum_{kk'} \sum_{\sigma\sigma'} c_{ik\sigma}^\dagger \hat{\tau}_{\sigma\sigma'} c_{jk'\sigma'}, \hat{\tau}_{\sigma\sigma'}$ are the components of the three Pauli matrices.

The total $SO(5)$ multiplet of width $\Delta_{SO(5)}$ determines

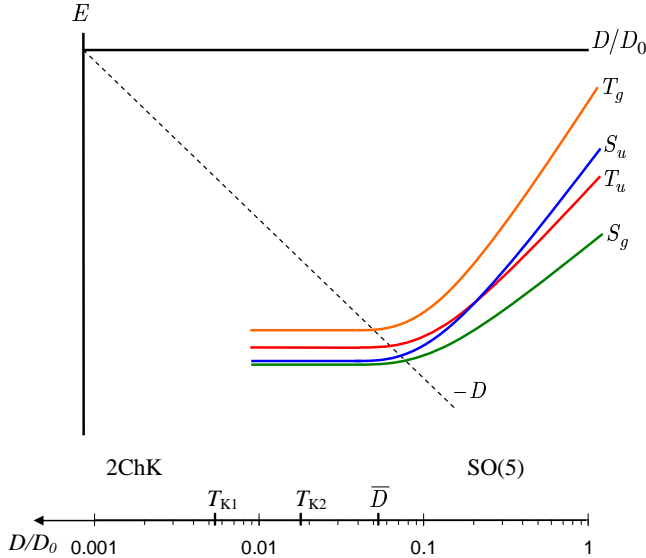


FIG. 2: (Color online) Upper panel: Energy levels in doubly occupied TQD renormalized within a scaling procedure. Lower panel: Logarithmic energy scale for a crossover from $SO(5)$ to two-channel KE as a function of scaling parameter $\eta = \ln D_0/D$.

tion of the eigenstates and eigenvalues of the Hamiltonian H_d). Within the energy scale of the bandwidth D (exceeding the width of this multiplet) the spectrum of the isolated TQD is characterized by $SO(8)$ dynamical symmetry. The dynamical symmetry group is formed by linear combinations of the operators $X^{\lambda\lambda'} = |\lambda\rangle\langle\lambda'|$ generating the spectrum of the Hamiltonian H_d (see¹⁴ for a regular description of dynamical symmetries). Hal-

the corresponding single-channel Kondo temperature¹⁶

$$T_{K1} = \bar{D} \exp \left(\frac{2}{j_1 + j_2 + \sqrt{(j_1 + j_2)^2 + 2\bar{j}_2^2}} \right), \quad (5)$$

provided $\bar{D} \gg T_{K1} \gg \Delta_{\text{SO}(5)}$. Here $j_i = \rho_0 J_i$, ρ_0 is the electron density of states on the Fermi level ε_F . This temperature is, however not universal: at the energy scale $D \lesssim \Delta_{\text{SO}(5)}$ the fine structure of the multiplet determines the Kondo scattering.

A two-channel orbital KE (2CKE) is possible in the situation shown in Fig. 2, where at $D < \bar{D}$ the two singlet levels $\bar{E}_{u,g}$, renormalized in accordance with Eq. (2), form an "orbital" doublet separated by a gap Δ_{TS} from the triplet \bar{E}_{Tu} . The conditions for such level crossing are discussed in the Appendix. In this configuration, the SW-like Hamiltonian can be written in terms of pseudospin Pauli matrices \vec{T} and $\vec{\tau}$ as,

$$\begin{aligned} H_{\text{orb}} = & -K_h \mathcal{T}_z + K_{\parallel} \mathcal{T}_z \sum_{\sigma} \tau_{z,\sigma} \\ & + \frac{K_{\perp}}{2} \left(\mathcal{T}^+ \sum_{\sigma} \tau_{\sigma}^- + \mathcal{T}^- \sum_{\sigma} \tau_{\sigma}^+ \right) \\ & - K_1 \mathcal{T}_z \sum_{kk'\sigma} (c_{e,k\sigma}^{\dagger} c_{e,k'\sigma} + c_{o,k\sigma}^{\dagger} c_{o,k'\sigma}) - K_2 \hat{I} \sum_{\sigma} \tau_{z,\sigma}. \end{aligned} \quad (6)$$

(see the Appendix for a definition of the parameters K_i). Here

$$\begin{aligned} \mathcal{T}^+ &= X^{S_g S_u}, \quad \mathcal{T}^- = X^{S_u S_g}, \\ \mathcal{T}_z &= \frac{X^{S_g S_g} - X^{S_u S_u}}{2}, \\ \hat{I} &= X^{S_g S_g} + X^{S_u S_u}, \\ \tau_{\sigma}^+ &= \sum_{kk'} c_{e,k\sigma}^{\dagger} c_{o,k'\sigma}, \quad \tau_{\sigma}^- = \sum_{kk'} c_{o,k\sigma}^{\dagger} c_{e,k'\sigma}, \\ \tau_{z,\sigma} &= \frac{1}{2} \left(\sum_{kk'} c_{e,k\sigma}^{\dagger} c_{e,k'\sigma} - \sum_{kk'} c_{o,k\sigma}^{\dagger} c_{o,k'\sigma} \right). \end{aligned} \quad (7)$$

The first term in the Hamiltonian (6) is an analog of the Zeeman term in the conventional KE. Its origin is the avoided level crossing $\bar{E}_{Su} - \bar{E}_{Sg} = K_h$ arising in the course of Haldane renormalization due to weak interchannel hybridization in the leads¹⁶. The spin-flip processes are absent in the singlet states. As a result the spin degeneracy is symmetry protected and the spin index is converted into the channel number. Thereby we arrive at a desirable situation, where spin projection quantum number plays the role of channel index and the two (orbital) channels are identical. This is the orbital 2CKE in an effective magnetic field $K_h/2$ ¹⁹. The channel isotropy is protected by spin-rotation symmetry of the singlet state.

The second stage of the RG procedure, that starts at the energy $\sim \bar{D} \gg \Delta_{TS}$ includes inter-channel Kondo cotunneling $\sim K_{\parallel}, K_{\perp}$, and indirect virtual processes via

excited triplet state $|T_u\rangle$ "inherited" from the first stage of the RG procedure derived from the Hamiltonian (3). The *full* system of scaling equations encoding the orbital KE is presented in the Appendix. Here we present the *reduced* system including the parameters relevant for the scale T^* characterizing the two-channel regime:

$$\begin{aligned} \frac{d\kappa_{\parallel\sigma}}{d \ln D} &= -\kappa_{\perp\sigma}^2 - 2\kappa_h \kappa_{2\sigma} - \frac{\bar{j}_2^2}{2} \\ &+ \frac{\kappa_{\parallel\sigma}}{4} \left[3(\kappa_{\parallel\uparrow}^2 + \kappa_{\parallel\downarrow}^2 + 2\kappa_h^2 \right. \\ &+ 4\kappa_{2\uparrow}^2 + 4\kappa_{2\downarrow}^2) + \kappa_{\perp\uparrow}^2 + \kappa_{\perp\downarrow}^2 \left. \right], \\ \frac{d\kappa_{\perp\sigma}}{d \ln D} &= -\kappa_{\parallel\sigma} \kappa_{\perp\sigma} - \frac{3\bar{j}_2^2}{4} \\ &+ \frac{\kappa_{\perp\sigma}}{4} \left[3(\kappa_{\parallel\uparrow}^2 + \kappa_{\parallel\downarrow}^2 + 2\kappa_h^2 \right. \\ &+ 4\kappa_{2\uparrow}^2 + 4\kappa_{2\downarrow}^2) + \kappa_{\perp\uparrow}^2 + \kappa_{\perp\downarrow}^2 \left. \right], \\ \frac{d\kappa_{2\sigma}}{d \ln D} &= -\frac{\kappa_h \kappa_{\parallel\sigma}}{2} \\ &+ \frac{\kappa_{2\sigma}}{4} \left[3(\kappa_{\parallel\uparrow}^2 + \kappa_{\parallel\downarrow}^2 + 2\kappa_h^2 \right. \\ &+ 4\kappa_{2\uparrow}^2 + 4\kappa_{2\downarrow}^2) + \kappa_{\perp\uparrow}^2 + \kappa_{\perp\downarrow}^2 \left. \right]. \end{aligned} \quad (8)$$

Here the 3rd order terms on the RHS are retained in accordance with the general theory of two-channel KE¹. The energy scale T^* is enhanced due to contribution from the enhanced parameter \bar{j}_2 . The coordinates of the corresponding fixed point are

$$\begin{aligned} \kappa_{\parallel\uparrow} &= \kappa_{\parallel\downarrow} = \frac{1 + \sqrt{1 + 2[\bar{j}_2^2 - 10\kappa_h^2]}}{4} \approx \\ &\approx \frac{1}{2} + \frac{\bar{j}_2^2}{4} - \frac{5}{2}\kappa_h^2, \\ \kappa_{\perp\uparrow} &= \kappa_{\perp\downarrow} = \sqrt{\kappa_{\parallel\uparrow}^2 - \kappa_h^2 - 0.5\bar{j}_2^2}, \\ \kappa_{2\uparrow} &= \kappa_{2\downarrow} = \frac{\kappa_h}{2}. \end{aligned} \quad (9)$$

In this way we arrive at the two-channel Hamiltonian with pseudospin operator as a source of Kondo screening and spin indices enumerating screening channels. The Zeeman operator is relevant for the 2CKE, and its influence on the scaling behavior in the nearest vicinity of the quantum critical point may be described within conformal field framework¹⁹. A peculiar feature of the orbital 2CKE described here is the multistage renormalization of the parameters of the bare Anderson Hamiltonian followed by an appropriate modification of the dynamical symmetry shared by the spectrum of the doubly occupied TQD as displayed in (Fig. 2).

The present scenario of orbital 2CKE implies peculiar behavior of various observables, such as the temperature dependence of the tunneling conductance $G(T)$. It is essentially distinct from the analogous behavior of $G(T)$ in the "conventional" spin 2CKE. First, in the weak coupling regime $T \gg \Delta_{\text{SO}(5)}$ ¹⁶, Kondo co-tunneling in the orbital KE occurs according to the *single* channel scenario. Two channel over-screening occurs only

at the strong coupling regime $T \ll \Delta_{\text{SO}(5)}$, where the crossover to NFL phase takes place. Second, in the orbital 2CKE, the Kondo temperatures in the weak and strong coupling regimes are essentially different parameters, whereas in the spin 2CKE the two scales are nearly the same, $T^* = \alpha T_{K2}$, where $\alpha \lesssim 1$ (see, e.g.,^{2,19}). Therefore the two asymptotic regimes for $G(T)$ are

$$G(0)/G_0 \sim \begin{cases} \ln^{-2}(T/T_{K1}), & T \gg T_{K1} \\ \frac{1}{2} + \sqrt{T/T^*}, & T \ll T^* \end{cases} \quad (10)$$

Numerical estimates of the RG parameters using

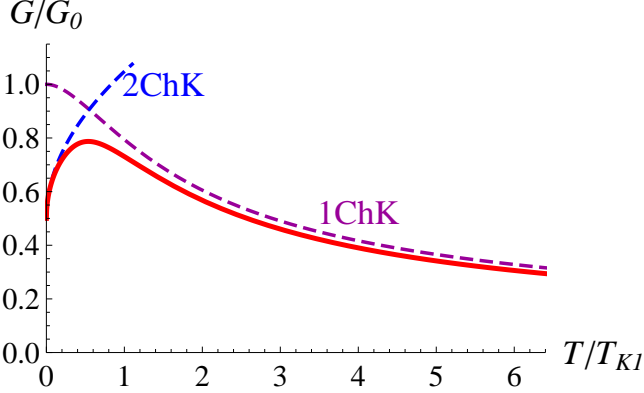


FIG. 3: (Color online) Temperature dependence of tunneling conductance (solid curve). Low- T orbital 2CKE and high- T 1CKE spin $\text{SO}(5)$ asymptotics are shown by the dashed curves. The input parameters are specified in the text

input values of the energy intervals $\Delta_{T_g, S_u} = 0.03$, $\Delta_{S_u, T_u} = 0.015$, $\Delta_{T_u, S_g} = 0.056$ (all in units of D_0) show that the Haldane RG transformation stops at $\bar{D}/D_0 = 0.053$ (the dependence $\bar{D}(\Lambda)$ is neglected in this estimate). As is known^{15,16}, the Kondo temperature for CQD displaying $\text{SO}(n)$ symmetry is non-universal and depends on the width of the corresponding multiplet. In our estimate $T_{K1}(\Delta_{\text{SO}(5)}) = 0.0054D_0$. On the other hand, the two-channel Kondo temperature T_{K2} found from Eqs. (8) without 3-rd order terms on the RHS is $T_{K2} = 0.018D_0 \gg T_{K1}$. The reasons for such strong enhancement are (i) the inequality $T_{K1}(\Delta_{\text{SO}(5)}) \ll T_{K1}(0)$ ¹⁶, (ii) the contribution of the enhanced parameter \tilde{j}_2 to the first two equations in the system (8): in accordance with our numerical calculations $\tilde{j}_2/\tilde{j}_1 \approx 1.5$, hence $T^*/T_{K1} \gg 1$.

This result may be compared with the situation arising in doubly occupied DQD in the serial geometry without source - drain symmetry, where the difference between the high-energy and low energy scales is related to the crossover from single channel KE to 2CKE due to asymmetry between the source/dot and drain/dot coupling²⁰. The crossover mechanism 1CKE \rightarrow 2CKE is different in that case (two-stage Kondo screening of two spins $\mathbf{S}_{(s,d)}$ attached to two electrodes with essentially differing Kondo scales $T_{Ks} \gg T_{Kd}$ ²¹). The 1CKE is characterized by the scale T_{Ks} , and the 2CKE regime

arises at essentially lower temperature $T_{K2} \ll T_{Ks}$ due to overscreening of the remaining spin 1/2 by the remaining electrons in the source and drain leads. Comparing the two mechanisms, we see that unlike²⁰, our mechanism leads to enhancement of the Kondo scale in the crossover 1CKE \rightarrow 2CKE.

In conclusion, we demonstrate that the transformation of the conventional high-temperature 1-channel spin-Kondo effect into unconventional low-temperature 2-channel orbital Kondo effect, where spin enumerates the screening channels, is possible in doubly occupied parallel TQD. The mechanism of this transformation is related to the singlet-triplet level crossing (Fig. 2). The necessary precondition for such crossover is the presence of at least two spin singlets in the low-energy spectrum of CQD, so that the minimal symmetry group is $\text{SO}(5)$. In case of TQD with $N = 2$ the low-energy spectrum is formed by $\text{SO}(8)$ two-triplets/two singlets multiplet. The theory is developed for the $\text{SO}(5)$ case, but the generalization for higher n is straightforward. Remarkable feature of this mechanism is the effect of enhancement of the 2CK Kondo temperature in comparison with that for 1CK regime. This effect is robust because the former "inherits" the Kondo cloud from the latter. The quantum critical point 2CKE-1CKE may also be achieved using the mutual disposition of the pairs $E_{T_u, g}$ and $E_{S_u, g}$ (Fig. 2) governed by the Coulomb blockade energies (see Appendix) as control parameters. With reasonable effort, the experimental techniques reported in Ref. (13) can be modified and employed to test the present prediction.

Acknowledgement The research of T.K and Y.A is partially supported by an ISF grant 173/2008.

Appendix A

1. Eigenstates of doubly occupied symmetric TQD

The Hamiltonian of the isolated isosceles TQD is:

$$\begin{aligned} H_d = & \sum_{a=l,r,c} \sum_{\sigma} \varepsilon_a d_{a\sigma}^{\dagger} d_{a\sigma} \\ & + \sum_a Q_a n_{a\uparrow} n_{a\downarrow} + \sum_{i=l,r} Q_{ic} n_{i\uparrow} n_{c\downarrow} \\ & + W \sum_{i\sigma} (d_{c\sigma}^{\dagger} d_{i\sigma} + H.c.). \end{aligned} \quad (A1)$$

Here ε_a are the energy level positions in the central (c) and side (l, r) wells of TQD, Q_a and Q_{ic} are intradot and interdot Coulomb blockade parameters, respectively, W is the tunneling integral between the central and side wells. We will be interested in the completely symmetric case, $\varepsilon_l = \varepsilon_r \equiv \varepsilon$, $Q_l = Q_r \equiv Q \ll Q_c$ and $Q_{lc} = Q_{rc} \equiv Q_{ic}$.

The Hamiltonian (A1) can be diagonalized by using

the basis of two-electron wave functions

$$\begin{aligned}
|s_i\rangle &= \frac{1}{\sqrt{2}} \left(d_{i\uparrow}^+ d_{c\downarrow}^+ - d_{i\downarrow}^+ d_{c\uparrow}^+ \right) |0\rangle, \\
|t_i, 1\rangle &= d_{i\uparrow}^+ d_{c\uparrow}^+ |0\rangle, \\
|t_i, 0\rangle &= \frac{1}{\sqrt{2}} \left(d_{i\uparrow}^+ d_{c\downarrow}^+ + d_{i\downarrow}^+ d_{c\uparrow}^+ \right) |0\rangle, \\
|t_i, \bar{1}\rangle &= d_{i\downarrow}^+ d_{c\downarrow}^+ |0\rangle, \\
|ex_i\rangle &= d_{i\uparrow}^+ d_{i\downarrow}^+ |0\rangle, \quad |ex_c\rangle = d_{c\uparrow}^+ d_{c\downarrow}^+ |0\rangle, \\
|ex_{lr}\rangle &= \frac{1}{\sqrt{2}} \left(d_{l\uparrow}^+ d_{r\downarrow}^+ - d_{l\downarrow}^+ d_{r\uparrow}^+ \right) |0\rangle, \\
|ex_{lr}^t, 1\rangle &= d_{l\uparrow}^+ d_{r\uparrow}^+ |0\rangle, \\
|ex_{lr}^t, 0\rangle &= \frac{1}{\sqrt{2}} \left(d_{l\uparrow}^+ d_{r\downarrow}^+ + d_{l\downarrow}^+ d_{r\uparrow}^+ \right) |0\rangle, \\
|ex_{lr}^t, \bar{1}\rangle &= d_{l\downarrow}^+ d_{r\downarrow}^+ |0\rangle.
\end{aligned} \tag{A2}$$

In this basis, the Hamiltonian (A1) is decomposed into singlet and triplet matrices,

$$\begin{aligned}
H_s &= \begin{pmatrix} \tilde{\varepsilon} & 0 & W & \sqrt{2}W & 0 & \sqrt{2}W \\ 0 & \tilde{\varepsilon} & W & 0 & \sqrt{2}W & \sqrt{2}W \\ W & W & 2\varepsilon & 0 & 0 & 0 \\ \sqrt{2}W & 0 & 0 & 2\varepsilon + Q & 0 & 0 \\ 0 & \sqrt{2}W & 0 & 0 & 2\varepsilon + Q & 0 \\ \sqrt{2}W & \sqrt{2}W & 0 & 0 & 0 & 2\varepsilon_c + Q_c \end{pmatrix}, \\
H_t &= \begin{pmatrix} \tilde{\varepsilon} & 0 & W \\ 0 & \tilde{\varepsilon} & -W \\ W & -W & 2\varepsilon \end{pmatrix},
\end{aligned} \tag{A3}$$

where $\tilde{\varepsilon} = \varepsilon_c + \varepsilon + Q_{ic}$.

The low-energy multiplet of two-electron states is:

$$\begin{aligned}
E_{S_g} &= \tilde{\varepsilon} - \frac{2W^2}{\Delta} - \frac{2W^2}{\Delta + Q} - \frac{4W^2}{\varepsilon_c + Q_c - Q_{ic} - \varepsilon}, \\
E_{T_u} &= \tilde{\varepsilon} - \frac{2W^2}{\Delta}, \\
E_{S_u} &= \tilde{\varepsilon} - \frac{2W^2}{\Delta + Q}, \\
E_{T_g} &= \tilde{\varepsilon},
\end{aligned} \tag{A4}$$

with $\Delta = \varepsilon - \varepsilon_c - Q_{ic}$.

The eigenfunctions corresponding to the energies (A4)

are

$$\begin{aligned}
|S_g\rangle &= \alpha_g \frac{|s_l\rangle + |s_r\rangle}{\sqrt{2}} - \beta_1 |ex_{lr}\rangle \\
&\quad - \beta_2 \frac{|ex_l\rangle + |ex_r\rangle}{\sqrt{2}} - \beta_3 |ex_c\rangle, \\
|T_u\rangle &= \alpha^T \frac{|t_l\rangle - |t_r\rangle}{\sqrt{2}} - \beta_1 |ex_{lr}^T\rangle, \\
|S_u\rangle &= \alpha_u \frac{|s_l\rangle - |s_r\rangle}{\sqrt{2}} - \beta_2 \frac{|ex_l\rangle - |ex_r\rangle}{\sqrt{2}}, \\
|T_g\rangle &= \frac{|t_l\rangle + |t_r\rangle}{\sqrt{2}},
\end{aligned} \tag{A5}$$

where

$$\beta_1 = \sqrt{2}W/\Delta, \quad \beta_2 = \sqrt{2}W/(\Delta + Q),$$

$$\beta_3 = \sqrt{2}W/(\varepsilon_c + Q_c - Q_{ic} - \varepsilon),$$

$$\alpha_g = \sqrt{1 - \beta_1^2 - \beta_2^2 - \beta_3^2},$$

$$\alpha^T = \sqrt{1 - \beta_1^2}, \quad \alpha_u = \sqrt{1 - \beta_2^2}.$$

Thus the lowest state of the isolated TQD is E_{S_g} . It is seen from (A4) that the singlet and triplet states alternate: $E_{S_g} < E_{T_u} < E_{S_u} < E_{T_g}$. The effective RG procedure renormalizing the eigenvalues of quantum dot once it is attached the leads¹⁷, has been generalized for multi-level TQD in Ref. 16. In accordance with this procedure, the levels E_Λ move downward as a function of the scaling parameter $\eta = \ln(D/D_0)$ with different slopes $\propto \Gamma_\Lambda$. The tunneling rates Γ_Λ for even and odd states (A5) obey the following hierarchy: $\Gamma_{T_g} > \Gamma_{S_u} > \Gamma_{T_u} > \Gamma_{S_g}$. This means that multiple level crossing is possible in the course of RG evolution. Besides, the pairs $E_{T_u, g}$ and $E_{S_u, g}$ are subject to level repulsion provided the left and right tunneling channels are not completely independent.

The flow evolution of each level stops at $E_\Lambda \approx \bar{D}$. The value \bar{D} is specific for each of the four levels. At this point the SW transformation leads to the Kondo Hamiltonian, and the Kondo-stage of RG procedure starts in accordance with the poor man scaling procedure.¹⁸ The phase diagram is quite complicated, because the two singlet and two triplet levels can intersect in several ways depending on the values of the model parameters $W, \tilde{\varepsilon}, \Delta, Q, Q_c, Q_{ic}$. Among these scenarios are: (I) S=1 Kondo regime corresponding to the scenario where T_g is the ground state, and the flow pattern of dynamical symmetries with the RG procedure is $SO(8) \rightarrow SO(5) \rightarrow SO(4) \rightarrow SO(3)$ (cf. the case of TQD with $N = 4$ studied in Ref. 16); (II) Absence of KE corresponding to the scenario where S_g is the ground state; (III) Orbital KE with almost degenerate S_g, S_u ground state. Here we focus on two competing phases, namely $SO(5)$ configuration, which involves two

singlet states and one triplet state, and orbital $SU(2)$ configuration, where two singlets form (quasi) degenerate pair and the triplet state is involved as a relatively soft excitation above this doublet.

The singlets S_g and S_u will be the lowest (renormalized) states in the SW limit, i.e., $\bar{E}_{S_g} = \bar{E}_{S_u} - 2K_h < \bar{E}_{T_g}, \bar{E}_{T_u}$, when:

$$\begin{aligned} \frac{2W^2\beta_2^2}{\beta_1^2 + \beta_3^2} \left(\frac{1}{\Delta} + \frac{2}{\varepsilon_c + Q_c - Q_{ic} - \varepsilon} \right) &< \frac{2W^2}{\Delta + Q} - K_h, \\ \frac{2W^2Q}{\Delta(\Delta + Q)} &< \\ &< \frac{2W^2(\beta_1^2 - \beta_2^2)}{\beta_1^2 + \beta_3^2} \left(\frac{1}{\Delta} + \frac{2}{\varepsilon_c + Q_c - Q_{ic} - \varepsilon} \right) - K_h. \end{aligned} \quad (A6)$$

Here $K_h/2 = \bar{M}_{lr}$ is the indirect tunneling amplitude between the side dots via the central dot and the leads arising in the course of renormalization¹⁶ [see also Eq. (A21) below].

2. $SO(5)$ -symmetry

When the two singlets $|S_\eta\rangle$ and the triplet $|T_u, \mu\rangle$ are almost degenerate, the exchange Hamiltonian can be written as a sum of spin and orbital parts:

$$H = H_{spin} + H_{orb}. \quad (A7)$$

The first term in Eq.(A7) describes the singlet-triplet transitions:

$$\begin{aligned} H_{spin} = \sum_{\mu} \bar{E}_{T_u T_u} X^{T_u T_u} + \sum_{S_\eta} \bar{E}_{S_\eta} X^{S_\eta S_\eta} \\ + J_{1u}^T \mathbf{S}_u \cdot \mathbf{s}_u + J_{1u}^{ST} \mathbf{R}_u \cdot \mathbf{s}_u + J_{2u}^{ST} (\mathbf{R}_{ug}^{(1)} \cdot \mathbf{s}_{gu} + \mathbf{R}_{gu}^{(2)} \cdot \mathbf{s}_{ug}). \end{aligned} \quad (A8)$$

Here $E_{S_{g/u}}(\bar{D}) = E_S \mp \bar{\Delta}_\Lambda$ and the effective exchange constants are

$$\begin{aligned} J_{1u}^T &= \frac{\alpha_T^2 V^2}{\varepsilon_F - \varepsilon}, & J_{1g}^{ST} &= -\frac{\alpha_g V^2}{\varepsilon_F - \varepsilon}, \\ J_{1u}^{ST} &= -\frac{\alpha_u \alpha_T V^2}{\varepsilon_F - \varepsilon}, & J_{2u}^{ST} &= -\frac{\alpha_g \alpha_T V^2}{\varepsilon_F - \varepsilon}. \end{aligned} \quad (A9)$$

The spherical components of the vector operators \mathbf{S}_u , \mathbf{R}_u , $\mathbf{R}_{ug}^{(1)}$ and $\mathbf{R}_{gu}^{(2)}$ are defined via Hubbard operators

connecting different states of the octet,

$$\begin{aligned} S_u^+ &= \sqrt{2}(X^{1_u 0_u} + X^{0_u \bar{1}_u}), \quad S_u^- = (S_u^+)^\dagger, \\ S_u^z &= X^{1_u 1_u} - X^{\bar{1}_u \bar{1}_u}, \\ R_u^+ &= \sqrt{2}(X^{1_u S_u} - X^{S_u \bar{1}_u}), \quad R_u^- = (R_u^+)^\dagger, \\ R_u^z &= -(X^{0_u S_u} + X^{S_u 0_u}), \\ R_{ug}^{(1)+} &= \sqrt{2}X^{1_u S_g}, \quad R_{ug}^{(1)-} = (R_{ug}^{(1)+})^\dagger, \\ R_{ug}^{(1)z} &= -X^{0_u S_g}, \\ R_{gu}^{(2)+} &= -\sqrt{2}X^{S_g \bar{1}_u}, \quad R_{gu}^{(2)-} = (R_{gu}^{(2)+})^\dagger, \\ R_{gu}^{(2)z} &= -X^{S_g 0_u}. \end{aligned} \quad (A10)$$

The spin operators for the electrons in the leads are introduced by the obvious relations

$$\begin{aligned} \mathbf{s}_g &= \frac{1}{2} \sum_{kk'} \sum_{\sigma\sigma'} c_{gk\sigma}^\dagger \hat{\tau}_{\sigma\sigma'} c_{gk'\sigma'}, \\ \mathbf{s}_u &= \frac{1}{2} \sum_{kk'} \sum_{\sigma\sigma'} c_{uk\sigma}^\dagger \hat{\tau}_{\sigma\sigma'} c_{uk'\sigma'}, \\ \mathbf{s}_{gu} &= \frac{1}{2} \sum_{kk'} \sum_{\sigma\sigma'} c_{gk\sigma}^\dagger \hat{\tau}_{\sigma\sigma'} c_{uk'\sigma'}, \quad \mathbf{s}_{ug} = (\mathbf{s}_{gu})^\dagger \end{aligned} \quad (A11)$$

The Hamiltonian (A8) possesses an $SO(5)$ symmetry. The group generators of the o_5 algebra are the vectors $\mathbf{S}_u, \mathbf{R}_u$ from (A10), the operators intermixing g - and u -states, namely, the vector $\tilde{\mathbf{R}} = \mathbf{R}_{ug}^{(1)} + \mathbf{R}_{gu}^{(2)}$,

$$\begin{aligned} \tilde{R}^+ &= \sqrt{2}(X^{1_u S_g} - X^{S_g \bar{1}_u}), \\ \tilde{R}^- &= (\tilde{R}^+)^\dagger, \\ \tilde{R}^z &= -(X^{0_u S_g} + X^{S_g 0_u}), \end{aligned} \quad (A12)$$

and the scalar operators A interchanging g, u variables of the degenerate singlets:

$$A = i(X^{S_u S_g} - X^{S_g S_u}). \quad (A13)$$

Additional vertices appear in the effective spin Hamiltonian (A8) at the second stage of Haldane-Anderson scaling procedure.^{17,18} As a result, the exchange part of the Hamiltonian (3) takes the form

$$\begin{aligned} H_{cot} &= J_1 \mathbf{S}_u \cdot \mathbf{s}_u + J_2 \mathbf{R}_u \cdot \mathbf{s}_u + J_3 (\mathbf{R}_{ug}^{(1)} \cdot \mathbf{s}_{gu} + \mathbf{R}_{gu}^{(2)} \cdot \mathbf{s}_{ug}) \\ &+ J_4 \mathbf{S}_u \cdot \mathbf{s}_g + J_5 \tilde{\mathbf{R}} \cdot \mathbf{s}_u \\ &+ J_6 (\mathbf{R}_{1g} \cdot \mathbf{s}_{ug} + \mathbf{R}_{2g} \cdot \mathbf{s}_{gu}) + J_7 \mathbf{S}_u \cdot (\mathbf{s}_{gu} + \mathbf{s}_{ug}) \\ &+ J_8 (\mathbf{R}_{ug}^{(1)} \cdot \mathbf{s}_{ug} + \mathbf{R}_{gu}^{(2)} \cdot \mathbf{s}_{gu}) \\ &+ J_9 \mathbf{R}_u \cdot \mathbf{s}_g + J_{10} \tilde{\mathbf{R}} \cdot \mathbf{s}_g + J_{11} \mathbf{R}_u \cdot (\mathbf{s}_{gu} + \mathbf{s}_{ug}) \\ &+ J_{12} (\mathbf{R}_{1g} \cdot \mathbf{s}_{gu} + \mathbf{R}_{2g} \cdot \mathbf{s}_{ug}), \end{aligned} \quad (A14)$$

where $\mathbf{R}_{1l} = X^{S_l S_r} \tilde{\mathbf{R}}_1$, $\mathbf{R}_{2l} = \tilde{\mathbf{R}}_2 X^{S_r S_l}$. The coupling constants in the Hamiltonian (A14) are subject to renor-

malization. Their values (A9) with

$$\begin{aligned} J_1(\bar{D}) &= J_{1u}^T, & J_2(\bar{D}) &= J_{1u}^{ST}, \\ J_3(\bar{D}) &= J_{2u}^{ST}, & J_i(\bar{D}) &= 0 \quad (i = 4 - 12) \end{aligned} \quad (\text{A15})$$

are taken as initial conditions for solving the scaling equations. These equations can be written in the following form:

$$\begin{aligned} \frac{dj_1}{d \ln d} &= -[j_1^2 + j_2^2 + j_5^2 + j_7^2 + j_{11}^2 + j_{11}(j_6 + j_{12}) \\ &\quad + \frac{j_3^2 + j_6^2 + j_8^2 + j_{12}^2}{2}], \\ \frac{dj_2}{d \ln d} &= -[2(j_1 j_2 + j_7 j_{11}) + j_7(j_6 + j_{12}) - m_{lr} j_5], \\ \frac{dj_3}{d \ln d} &= -[j_3(j_1 + j_4) + j_7(j_5 + j_{10}) - m_{lr}(j_6 + j_{11})], \\ \frac{dj_4}{d \ln d} &= -[j_4^2 + j_7^2 + j_9^2 + j_{10}^2 + j_{11}^2 + j_{11}(j_6 + j_{12}) \\ &\quad + \frac{j_3^2 + j_6^2 + j_8^2 + j_{12}^2}{2}], \\ \frac{dj_5}{d \ln d} &= -[2j_1 j_5 + j_7(j_3 + j_8) - m_{lr} j_2], \\ \frac{dj_6}{d \ln d} &= -[j_6(j_1 + j_4) - m_{lr} j_3], \\ \frac{dj_7}{d \ln d} &= -\left[\frac{(j_3 + j_8)(j_5 + j_{10}) + (j_2 + j_9)(j_6 + j_{12})}{2}\right. \\ &\quad \left.+ j_7(j_1 + j_4) + j_{11}(j_2 + j_9)\right], \\ \frac{dj_8}{d \ln d} &= -[j_8(j_1 + j_4) + j_7(j_5 + j_{10}) - m_{lr}(j_{11} + j_{12})], \\ \frac{dj_9}{d \ln d} &= -[2(j_4 j_9 + j_7 j_{11}) + j_7(j_6 + j_{12}) - m_{lr} j_{10}], \\ \frac{dj_{10}}{d \ln d} &= -[2j_4 j_{10} + j_7(j_3 + j_8) - m_{lr} j_9], \\ \frac{dj_{11}}{d \ln d} &= -[j_{11}(j_1 + j_4) + j_7(j_2 + j_9)], \\ \frac{dj_{12}}{d \ln d} &= -[j_{12}(j_1 + j_4) - m_{lr} j_8]. \end{aligned} \quad (\text{A16})$$

where $j_i = \rho_0 J_i$ ($i = 1, \dots, 12$), $d = \rho_0 D$ and $m_{lr} = \rho_0 \bar{M}_{lr}$.

From equations (A16), one deduces the Kondo temperature,

$$T_{K2} = \bar{D} \left(1 - \frac{2\sqrt{2}m_{lr}}{j_1 + j_2 + \sqrt{(j_1 + j_2)^2 + 2j_3^2}} \right) \frac{1}{\sqrt{2}m_{lr}} \quad (\text{A17})$$

which transforms to Eq. (5) of the main text at $m_{lr} \rightarrow 0$.

3. Orbital KE

The singlets S_g and S_u become the lowest renormalized states in the SW limit, i.e., $\bar{E}_{S_g} = \bar{E}_{S_u} - 2\bar{M}_{lr} < \bar{E}_{T_g}, \bar{E}_{T_u}$,

when:

$$\begin{aligned} \frac{2W^2\beta_2^2}{\beta_1^2 + \beta_3^2} \left(\frac{1}{\Delta} + \frac{2}{\varepsilon_c + Q_c - Q_{ic} - \varepsilon} \right) &< \frac{2W^2}{\Delta + Q} - \bar{M}_{lr}, \\ \frac{2W^2Q}{\Delta(\Delta + Q)} &< \\ &< \frac{2W^2(\beta_1^2 - \beta_2^2)}{\beta_1^2 + \beta_3^2} \left(\frac{1}{\Delta} + \frac{2}{\varepsilon_c + Q_c - Q_{ic} - \varepsilon} \right) - \bar{M}_{lr}. \end{aligned} \quad (\text{A18})$$

In this case the two-channel orbital Kondo effect can be realized. The corresponding cotunneling Hamiltonian has the form:

$$\begin{aligned} H_{\text{orb}} &= \bar{M}_{lr}(X^{uu} - X^{gg}) \\ &+ \frac{\alpha_g^2}{2} \frac{V^2}{\varepsilon_F - \varepsilon} \sum_{kk'\sigma} X^{S_g S_g} c_{e,k\sigma}^\dagger c_{e,k'\sigma} \\ &+ \frac{\alpha_u^2}{2} \frac{V^2}{\varepsilon_F - \varepsilon} \sum_{kk'\sigma} X^{S_u S_u} c_{o,k\sigma}^\dagger c_{o,k'\sigma} \\ &+ \frac{\alpha_g \alpha_u}{2} \frac{V^2}{\varepsilon_F - \varepsilon} \sum_{kk'\sigma} (X^{S_g S_u} c_{o,k\sigma}^\dagger c_{e,k'\sigma} + X^{S_u S_g} c_{e,k\sigma}^\dagger c_{o,k'\sigma}), \end{aligned} \quad (\text{A19})$$

with $c_{(e,o),k\sigma} = \frac{1}{\sqrt{2}}(c_{l,k\sigma} \pm c_{r,k\sigma})$, and avoided crossing of the singlet states taken into account. The Hamiltonian (A19) can be rewritten in terms of pseudospin Pauli matrices $\vec{\tau}$ and $\vec{\tau}$:

$$\begin{aligned} H_{\text{orb}} &= -K_h \mathcal{T}_z + K_{\parallel} \mathcal{T}_z \sum_{\sigma} \tau_{z,\sigma} \\ &+ \frac{K_{\perp}}{2} \left(\mathcal{T}^+ \sum_{\sigma} \tau_{\sigma}^- + \mathcal{T}^- \sum_{\sigma} \tau_{\sigma}^+ \right) \\ &- K_1 \mathcal{T}_z \sum_{kk'\sigma} (c_{e,k\sigma}^\dagger c_{e,k'\sigma} + c_{o,k\sigma}^\dagger c_{o,k'\sigma}) - K_2 \hat{I} \sum_{\sigma} \tau_{z,\sigma}. \end{aligned} \quad (\text{A20})$$

(see also Eqs. (6), (7) of the main text). The coupling constants are:

$$\begin{aligned} K_h &= 2\bar{M}_{lr}, \\ K_{\parallel} &= \frac{\alpha_g^2 + \alpha_u^2}{2} \frac{V^2}{\varepsilon_F - \varepsilon}, \\ K_{\perp} &= \frac{\alpha_g \alpha_u V^2}{\varepsilon_F - \varepsilon}, \\ K_1 &= K_2 = \frac{\alpha_g^2 - \alpha_u^2}{4} \frac{V^2}{\varepsilon_F - \varepsilon}. \end{aligned} \quad (\text{A21})$$

The anisotropic Hamiltonian (A20) describes two-channel orbital Kondo effect in an effective "magnetic field" K_h . The coupling constant K_h remains unrenormalized (because all the terms $\sim \tau_z^2$ contribute to K_1), but it affects the renormalization of the other coupling constants.

-
- ¹ P. Nozières and A. Blandin, J. Physique **41**, 193 (1980).
 - ² R.M. Potok, I.G. Rau, H. Shtrikman, Y. Oreg, and D. Goldhaber-Gordon, Nature **446**, 167 (2007).
 - ³ T. Kuzmenko, K. Kikoin, and Y. Avishai, Europhys. Lett. **64**, 218 (2003).
 - ⁴ J. Kondo, Physica **84B**, 40, 207 (1976).
 - ⁵ K. Vladár, A. Zawadowski, Phys. Rev. B **28**, 1564, 1582 (1983).
 - ⁶ D.L. Cox and A. Zawadowski, Adv. Phys. **47**, 943 (1998).
 - ⁷ Yu.M. Kagan and N.V. Prokof'ev, Sov. Phys. JETP **63**, 1276 (1986); **69**, 836 (1989).
 - ⁸ I.L. Aleiner, B.L. Altshuler, Y.M. Galperin, and T.A. Shutenko, Phys. Rev. Lett. **86**, 2629 (2001).
 - ⁹ I.L. Aleiner and D. Controzzi, Phys. Rev. B **66**, 045107 (2002).
 - ¹⁰ K.A. Matveev, Phys. Rev. B **51**, 1743 (1995).
 - ¹¹ E. Lebanon, A. Schiller, Phys. Rev. B **64**, 245338 (2001).
 - ¹² M. Arnold, T. Langenbruch, and J. Kroha, Phys. Rev. Lett. **99**, 186601 (2007).
 - ¹³ S. Amaha, T. Hatano, T. Kubo, S. Teraoka, Y. Tokura, S. Tarucha, and D.G. Austing, Appl. Phys. Lett. **94**, 092103 (2009).
 - ¹⁴ K. Kikoin, M.N. Kiselev and Y. Avishai, *Dynamical Symmetries for Nanostructures*, Springer, Wien 2012.
 - ¹⁵ K. Kikoin and Y. Avishai, Phys. Rev. Lett. **86**, 2090 (2001); Phys. Rev. B **65**, 115329 (2002).
 - ¹⁶ T. Kuzmenko, K. Kikoin, and Y. Avishai, Phys. Rev. Lett. **89**, 156602 (2002); Phys. Rev. B **69**, 195109 (2004).
 - ¹⁷ F. D. M. Haldane, Phys. Rev. Lett. **40**, 416 (1978).
 - ¹⁸ P.W. Anderson, J. Phys. C **3**, 2435 (1970).
 - ¹⁹ I. Affleck, J. Phys. Soc. Jpn. **74**, 59 (2005); Lecture Notes, Les Houches Summer School **89**, pp. 3-64 (2008).
 - ²⁰ A.K. Mitchell, E. Sela, and D.E. Logan, Phys. Rev. Lett. **108**, 086405 (2012).
 - ²¹ G. Zarand, C.-H. Chung, P. Simon, and M. Vojta, Phys. Rev. Lett. **97**, 166802 (2006).